Numerical Investigation on the Effects of the Setting of the Load Control System of a Formula SAE Single-Cylinder Turbocharged Engine on Fuel Efficiency and Performance

Numerical Investigation on the Effects of the Setting of the Load Control System of a Formula SAE Single-Cylinder Turbocharged Engine on Fuel Efficiency and Performance

S Raspanti[1], M Ciampolini[1], S Bigalli[2], A Fabiani[3], L Romani[1] and G Ferrara[1*]

[1] Department of Industrial Engineering, Università degli Studi di Firenze, via di Santa Marta 3, 50139 Firenze, Italy
[2] ATOP S.p.a., strada S. Appiano 8/A, 50028 Barberino Tavarnelle, Italy
[3] ALTEN Italia S.p.a., via Francesco Zanardi 2/7, 40131 Bologna, Italy

* Contact Author: giovanni.ferrara@unifi.it

Abstract. The target of motorsport has always been maximising the performance. Increasingly stringent rules on fuel usage, however, have moved the research on engine design and control rules toward efficiency enhancement. Turbocharging is a typical solution to match both targets; however, it suffers from the turbo-lag phenomenon, especially when the maximum power is limited by an air restrictor. In the present paper, an investigation on a combined solution aimed at contemporarily improving transient response and efficiency in FSAE events, both leading to a higher score, is carried out. In detail, the adoption of an anti-lag valve and an efficiency-based control schedule, markedly exploiting the wastegate actuator, is proposed in place of the classic combination blow-off valve and performance-based strategy. The analyses were carried out on the 520 cm^3 single-cylinder 4-stroke turbocharged engine of the Firenze Race Team. In order to predict the potential of the proposed load control solution, a predictive combustion engine model (which design process is exhaustively described in the paper), adopting the K-k-ε turbulence model, was developed in the GT-Suite software and calibrated by means of test-bench data and 3-D CFD analyses. A vehicle model, calibrated by means of telemetry data, was finally developed to compare the proposed solution to the baseline load control system in typical race conditions, showing benefits in terms of performance, drivability, and efficiency.

1. Introduction

Formula SAE (FSAE) is the main opportunity for students to exhibit their talents in the design and development of race car prototypes. FSAE regulations are constantly updating, becoming even more stringent. The most strict imposition is the adoption of an air restrictor, limiting the inlet airflow and thus, the maximum engine performance [1]. The restrictor should be efficiently designed, since a high pressure drop means a low air mass flow [2]. The regulation also imposes a limit on displacement (710 cm^3) and binds the sequence of components at the intake system, depending on the adoption of a super- or turbo-charging system. The regulation also focuses to driver safety and cost reduction.

A FSAE team can collect up to 1000 point per race, of which 325 are related to static events, 575 to dynamic events (acceleration, autocross, skid-pad, endurance), and the remainder to the fuel economy during the endurance session. This complex scenario leads a team not to focus on engine performance

only, but also on drivability, reliability, and fuel efficiency. In particular, the latter goes against the research of performance, as the presence of the air restrictor requires supercharging strategies and higher amounts of fuel in order to increase the engine torque [3].

If on a side, it is possible to operate on the combustion process in order to improve efficiency by means of innovative ignition systems [4], or even to implement electrically assisted turbochargers to improve transient response [5], on the other hand, the smart tuning of the load control system is the main methodology to achieve significant benefits without adding system complexity.

In gasoline turbocharged engines, as in the case of the Firenze Race Team (FRT), load is controlled by means of throttle body (TB) and waste-gate valve (WG). For the same amount of injected fuel and ignition advance, the same load can be achieved with a small volumetric flow (chocked TB) and a high boost pressure (closed WG) or with wider-open throttle conditions and a modulated WG. Thus, the choice on the actuation strategy relies on the intended use and the desired drivability.

The classic motorsport control schedule (performance-based, PBS) aims at opening the WG to limit the boost pressure to the maximum allowable value. Since load control in low-load condition lies on the TB, load variation is almost instantaneous, making it well-suited for quick transient responses; however, pumping losses increase in steady-state operations, since the TB modulation worsens the pressure drop in the intake manifold and the WG closure leads to a higher exhaust back-pressure.

On the contrary, the maximum engine efficiency would be achieved when WG is kept as open as possible to fulfil the load demand (efficiency-based schedule, EBS) [6], despite the transient response may not be enough rapid for race requirements. To improve the torque response at high loads while maintaining the efficiency benefits of the EBS schedule, a mid-region in which TB and WG are contemporarily actuated (three-region control) was proposed in [7]. However, a TISO controller for the coordinated region, as presented in [7], is difficult to be adopted in motorsport engine control modules (ECM), as in Formula SAE, so that a different actuation methodology is required.

The 2021 FRT's vehicle (FR-21T) propulsion system is based on a 520 cm^3 single-cylinder four-stroke (4S) spark-ignition (SI) port fuel injection (PFI) turbocharged prototype derived from a 498 cm^3 Betamotor engine for offroad application. The FR-21T implements an electronic TB and an electronic WG to control engine load. A PBS control strategy is uploaded on the ECU, aimed at maximizing the engine response during transients, thus promoting WG closure. The compressor is provided with a pneumatic blow-off valve (BOV) to protect compressor during TB closing, which however introduces sever losses due to the lack of compression energy exploitation.

To avoid energy losses and to improve transient response, the use of a by-pass valve (BPV, or anti-lag valve), in place of the pneumatic BOV, can be considered. In fact, the recirculation of compressed air may reduce the energy exchanged between compressor blades and airflow, keeping turbocharger at high rotation speeds. This feature has the potential to reduce turbo-lag, thus also improving drivability. Moreover, to achieve a better efficiency, a three-region EBS aimed at improving WG opening can be implemented, especially if a rapid transient response is favoured by the BPV.

This paper aims at evaluating the potential improvements that the simultaneous adoption of a BPV and an EBS (marked as EBS-BPV system) would bring in FSAE race conditions in comparison to the baseline PBS-BOV setup. To evaluate the proposed upgrading, the development of a detailed GT-Suite vehicle model capable of predicting engine behaviour and vehicle dynamics was required. Thus, an accurate model calibration was performed by using a wide set of experimental and 3-D CFD data.

Firstly, the paper shows the procedure followed to develop and validate the complex vehicle model, including test-bench tests, CFD analyses, and predictive combustion modelling. Then, it presents the feasibility study of the proposed solution, in which the potential benefits of adopting the EBS-BPV system are highlighted and discussed. The intermediate stages required to develop the predictive combustion model in the GT-Suite software are finally presented in Appendix.

2. Materials and method

In the present chapter the procedure followed to develop the numerical model of the FR-21T vehicle on the GT-Suite software is shown. The latter was required to reliably understand the feasibility of the

proposed load control solutions. Firstly, the main features of the FR-21T vehicle are presented. Then, the test-bench and CFD analyses, required to obtain the modelling data, are shown. Finally, the predictive combustion vehicle model is presented and validated.

2.1. Test case vehicle

The FR-21T is supported by an AISI 4130 steel tube trellis frame. Suspensions present a front and rear double wishbone geometry with anti-roll bars and push-rod kinematics for the shock absorbers. Hubs and uprights are made of 7075 aluminum alloy and support a braking system with four-piston calipers, coupled to 200 mm front and 190 mm rear discs. The vehicle, presented in figure 1a, is also equipped with carbon fiber front and rear wings to achieve low-speed downforce.

Since the 37kW 498 cm^3 stock Betamotor engine markedly decreases performance when applying the 20 mm restrictor, in order to restore volumetric efficiency, the displacement was upgraded to 520 cm^3 and a high-speed Honeywell MGT1238Z turbocharger was implemented. The aluminum alloy compressor impeller (72% max. efficiency at a compression ratio of 2.1 and 205000 rpm) presents a min. (max.) diameter of 22.5 (38.1) mm, and it is protected from rapid TB closures by means of a standard pneumatic BOV. The Inconel turbine impeller instead presents a min. (max.) diameter of 28.4 (35.5) mm, distributed on twelve blades, and the WG control is tuned to keep the turbine temperature below 980 °C to reduce thermal stresses. A heat exchanger is also put downstream of the compressor to avoid knocking phenomena while improving further volumetric efficiency. The resulting FRT turbocharged engine provides 55 kW at 8000 rpm and 60 Nm at 5500 rpm. The FR-21T powertrain is shown in figure 1b, while engine main characteristics are summarized in table 1.

Figure 1a. Render of the FR-21T vehicle.

Figure 1b. Render of the FR-21T powertrain.

Table 1. Main features of the FR21-T single-cylinder turbocharged engine.

Displacement [cm^3]	Bore [mm]	Stroke [mm]	CR [-]	Boost (max) [bar]	Torque (max) [Nm]
518	101.98	63.40	9.02:1	1.4	60

2.2. Load control

In the FR-21T engine the load request is primarily actuated via a 44 mm Bosch electronic TB, which target opening angle is a function of the pedal position. Actuation relies on the engine control module (ECM) by means of an H-bridge acting in feedback through a PID controller receiving the TPS signal.

Contemporarily, the boost pressure control is carried out by means of a PID controller which target depends on engine speed and throttle position. The signal of the manifold absolute pressure sensor (MAP) downstream of the TB is sent to the PID controller as input signal. Downstream of the PID controller, the target WG position is evaluated by adding a pre-calibrated value depending on the target boost pressure. The WG is controlled by means of linear actuator moved by a second H-bridge. The latter operates by means of a PID controller feedback controlled by measuring the actual position of the actuator itself. The operating flow of the boost pressure control system is presented in figure 2.

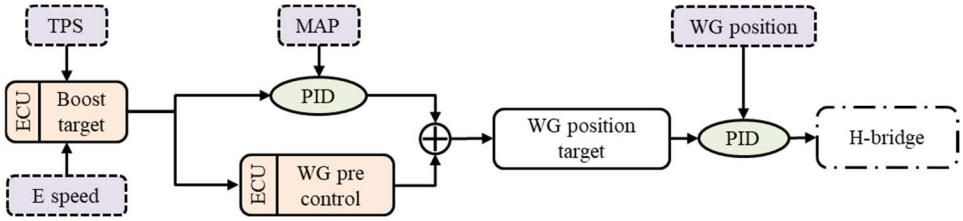

Figure 2. Operating scheme of the boost pressure control and actuation system.

The MAP signal is also used in the ECM, together with the engine load signal, to evaluate the required amount of fuel and the ignition timing advance through pre-calibrated maps.

The turbocharging system also presents a pneumatic BOV venting the compressed air returning from the TB to the compressor when it rapidly closes. Despite the reliability of this solution, it causes efficiency losses due to the ejection of compressed air.

A performance-based strategy (PBS), representing a typical motorsport setup, i.e., aimed at maximizing the transient response without accounting for fuel efficiency, is implemented on the ECM of the FR-21T. At low engine loads (region 1) the WG is closed, and the actuation relies on the TB only. At medium loads (region 2) instead most of the load control relies on the TB, while the WG starts to open; at high loads (region 3) finally the control relies entirely on the WG, since the TB is fully open. The performance-based strategy of the FR21-T is depicted in figure 3a, in which the blue continuous line represents the opening degree of the TB and the red dashed line that of the WG.

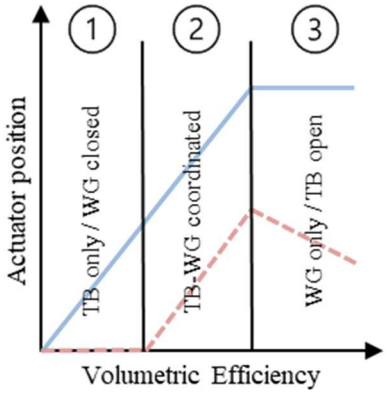

Figure 3a. Performance-based schedule, PBS.

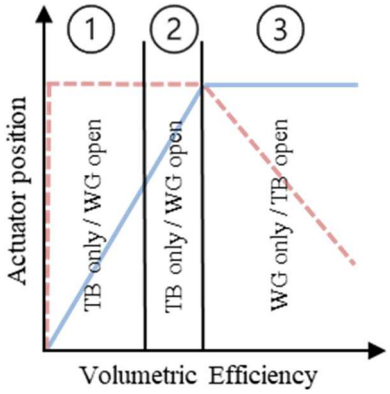

Figure 3b. Efficiency-based schedule, EBS (steady-state).

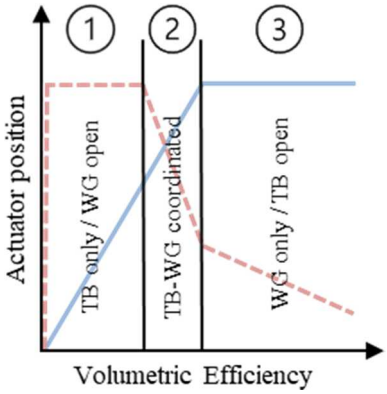

Figure 3c. Efficiency-based schedule, EBS (transient).

In view of the future FSAE competitions, the combined adoption of a BPV with an efficiency-based schedule (EBS-BPV system) was proposed to contemporarily improve transient response and efficiency. In fact, despite the higher complexity requiring a different sensors positioning [8], the recirculation of compressed air due to the BPV can reduce the energy exchanged between blades and airflow, thus maintaining the turbocharger at high speed and reducing turbo-lag intensity. Moreover, the design of a smart EBS aimed at reducing fuel usage is well-suited to improve the final score.

Contrarily to PBS systems, mainly relying on TB control, an EBS strategy tends to use a higher WG opening level to avoid the pressure drop across the TB and reduce backpressure [6]. In order to improve transients, a three-region EBS can be adopted [7]. In the proposed three-region EBS, in ideal steady-state conditions (figure 3b), in the 1st and 2nd regions, the WG valve is wide open while control is entrusted to TB. The main difference among them relates to the actioning of the boost control in the 2nd region to prepare the system to a transient condition. The 2nd region applies until 100% of the volumetric efficiency (VE) in WG wide open condition is achieved. Above that load request, TB is wide open, and the control is entrusted to the progressively closure of the WG.

In transient conditions (figure 3c) instead a coordinated control of TB and WG is required in the 2nd region. Thus, the 1st region applies until 80% of VE is achieved with wide open WG. Above this load request, the 2nd region, in which the boost pressure PID is activated (on the left of figure 2), and TB continues to gradually open, is applied. It is worth noting that the closing of the WG (slope of the curve) in the 2nd (but also 3rd) region depends on turbo-lag, thus figure 3c should be intended as an example. Finally, corresponding to the highest load requests, the 3rd region is applied, in which the TB is kept in wide-open position and the WG continues gradually to close.

It is worth noting that, in order to reduce the turbo-lag phenomenon, the EBS-BPV control system was paired to a null-injection WG actuation strategy for the gas pedal release phase only, in which the WG actuator is kept fully closed until the load request is lower than 1%, thus keeping the turbocharger at high speed. This feature can be observed in region 1 of figure 3b and 3c. This feature is also present, in itself, in the PBS schedule since the WG is kept closed in the entire first region.

2.3. Experimental test case

To evaluate the potential benefits of the proposed load control solution, a predictive vehicle model was required. The development of such tools crosses several phases, among which the experimental tests at the test bench represent the first step; in fact, the experimental in-cylinder pressure behaviour is used, at first, to develop the heat release curves of the imposed combustion model, then, together with the trend of intake and exhaust pressure, to characterize the TPA ("Three Pressure Analysis") model, and finally, to calibrate the parameters of the predictive combustion model. The experimental activity on the FRT's engine was carried out at the engine test facility of the Department of Industrial Engineering of the University of Florence. The engine was tested on a 110kW eddy current APICOM FR150 test bench. Torque and power were measured at the gearbox output. Full load conditions, between 6000 and 10500 rpm, were investigated. Both averaged and instantaneous measurements were carried out as required by the calibration procedure of the engine combustion models.

Concerning averaged measurements, fuel mass flow was measured through the AVL SORE PLU 110. The air-to-fuel ratio inside the combustion chamber was indirectly estimated by means of a Bosch LSU 4.9 lambda sensor coupled with an ETAS ES636.1 lambda module. K-type thermocouples were installed in the engine exhaust duct, and in the turbine inlet and outlet. Instead, T-type thermocouples were positioned downstream the restrictor, in the compressor outlet, downstream the throttle valve and in the intercooler outlet. Averaged pressure sensors were installed downstream of the air restrictor, compressor, throttle valve, and intercooler; even pressure upstream and downstream the turbine were measured. All the averaged measurements were acquired by means of the CoBa software, developed at Department of Industrial Engineering of the University of Florence, based on the NI cRIO platform.

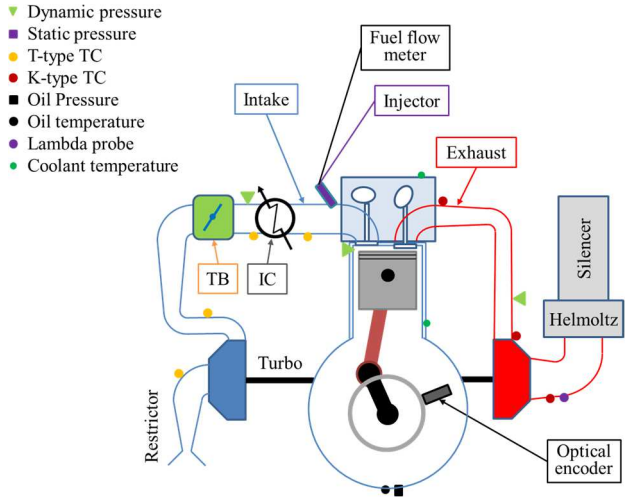

Figure 4a. Measurement system layout.

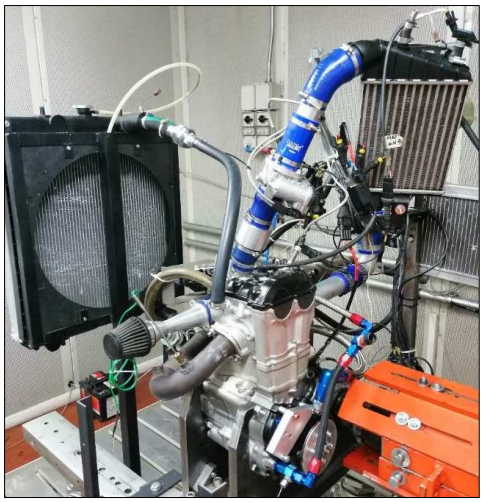

Figure 4b. FR-21T at the test bench.

With regards to instantaneous measurements, the AVL GR12D piezoelectric sensor was used to measure the in-cylinder pressure; intake and exhaust pressures were instead measured by means of a Kulite ETL-173 and a Kulite EWCTV-312M pressure transducers respectively. Sensors signals were triggered through an AVL 365X optical encoder (0.5 °CA resolution). Indicating data were acquired using the AVL IndiMicro system and processed through the AVL Indicom software.

The layout of the measurement system in shown in Figure 4a, in which dash dot lines refer to averaged pressure sensors, dash lines to instantaneous pressure sensors, linear and square dot lines to K-type and T-type thermocouples, respectively. Figure 4b instead shows the engine at the test bench.

2.4. CFD analysis

Indicating data are not enough to develop a predictive combustion model, since turbulence features (tumble and swirl number, turbulence kinetic energy, turbulence length scale) are required to calibrate the constants of the GT-Suite K-k-ε turbulence model to correctly predict the flame front development. Moreover, a valve tumble coefficient is required from engine modelling, for which experimental flow bench data must be known, despite they are usually missing. Thus, a 3-D CFD analysis was required.

In the present study the swirl number was not accounted since geometries of inlet ducts do not provide a significant swirled flow field. The CFD analysis was carried out using CONVERGE CFD. This solver self generates an orthogonal structured grid at runtime based on user-defined parameters. The turbulence flow is described by the unsteady Reynolds-averaged Navier-Stokes approach (U-RANS), while the k-ε RNG model was used for the turbulence modelling. The PISO algorithm was adopted to solve the pressure/velocity coupling, while the second order upwind scheme was set for spatial discretization. A variable time-step based on the definition of a maximum CFL was used. The computational domain is shown in Figure 5a.

The base grid size was set to 4 mm in the whole domain. Different techniques were used to control the element size without increasing the computational costs. A fixed embedding was used in the cylinder zone to refine the grid and to achieve a proper resolution of turbulence scales. An additional embedding in the valve zone was used to solve the flow field during valve opening. Furthermore, the adaptive mesh refinement (AMR), automatically refining the grid where the complex flow phenomena are established, was used. Figure 5b depicts the mesh grid, while settings are summarized in table 2.

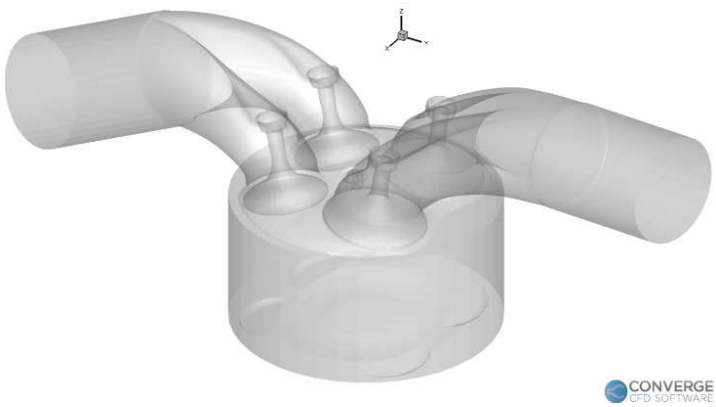

Figure 5a. CFD computational domain.

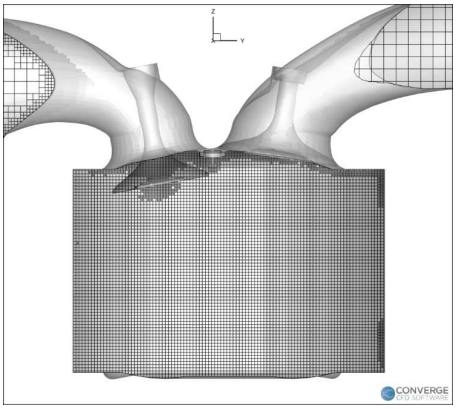

Figure 5b. Cylinder mesh grid.

Table 2. Mesh main characteristics.

Base grid size [mm]	Cylinder element size [mm]	Valves element size [mm]	In-cylinder elements at BDC	Max domain elements
4	1	0.5	$1.3*10^6$	$1.8*10^6$

To extract the turbulent parameters (tumble ratio, turbulent kinetic energy, turbulent length scale), a 3-D CFD analysis of the scavenging process were carried out at 6000 rpm, 8000 rpm and 10000 rpm. Simulations start before the exhaust valves opening (EVO). Figure 6a shows the in-cylinder pressure comparison between the 3-D CFD results and 1-D GT-Suite TPA (Three Pressure Analysis) model results (used as boundary conditions in input to the CFD) at 6000 rpm. The CFD results are quite accurate, and a good accuracy is achieved by the 3-D solver in predicting the in-cylinder pressure during the compression phase. Since the results at different rpm show a similar behaviour, only the results of in-cylinder pressure at 6000 rpm are shown in figure 6a.

As an example of CFD results, figure 6b shows the CFD results in terms of in-cylinder Turbulent Kinetic Energy (TKE) during the scavenging process. It is worth noting that the turbulent kinetic energy at 8000 rpm during the overlap phase is the highest, since thermodynamic effects are tuned. On the contrary, during the intake phase, the higher rotation speed and the higher TKE due to the stronger turbulent eddies.

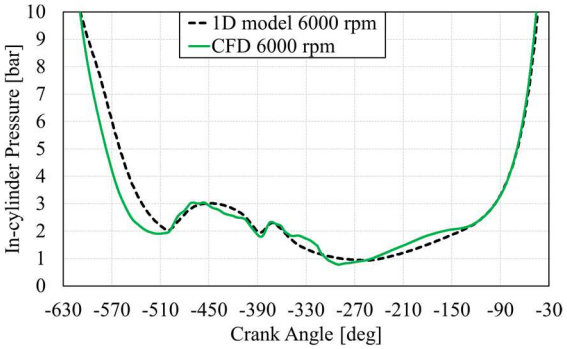

Figure 6a. Pressure trend at 6000 rpm (3-D CFD vs 1-D model).

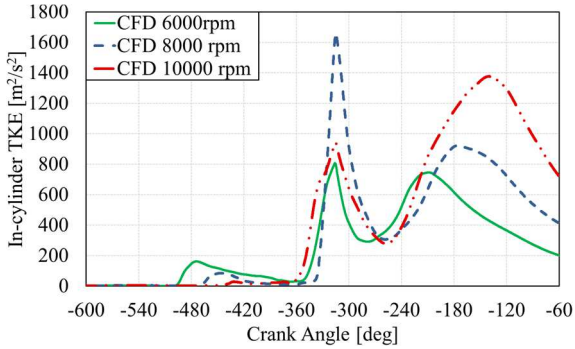

Figure 6b. Turbulent Kinetic Energy at 6000, 8000 and 10000 rpm from 3-D CFD simulations.

2.5. Engine and vehicle modelling

The model of the FR-21T was developed in the GT-Suite ambient. To reliably predict the effects of introducing new components and strategies aimed at improving the load control, a reliable prediction of combustion process behavior, as well as the temperature and pressure inside cylinder and ducts, was required. Since the 10-90% mass burnt fraction (MBF) duration is related to turbulence, the prediction of the trend of the turbulent kinetic energy (TKE), turbulence dissipation rate (ε), and length scale was also required. The development of a predictive combustion model is thus a complex process, for which the aforementioned experimental and CFD analyses were carried out.

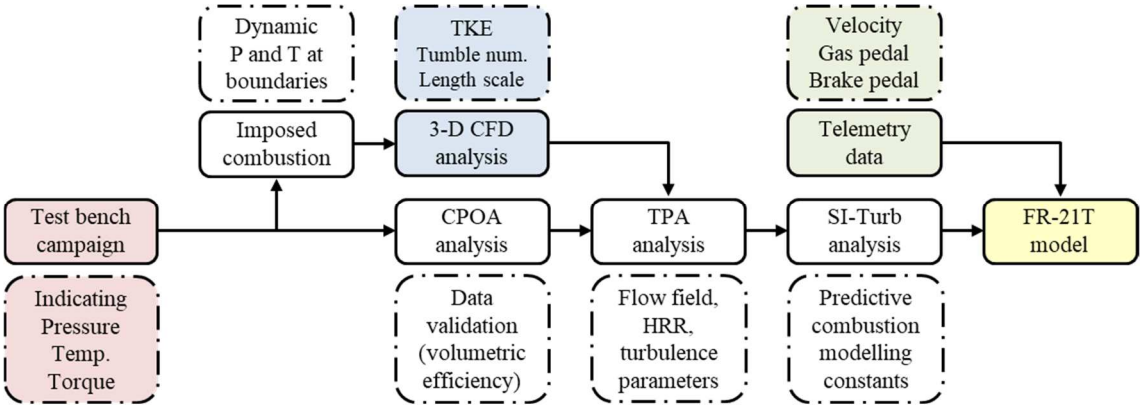

Figure 7. Modelling procedure for the development of the predictive combustion model.

The model development procedure involves the use of several GT-Suite subroutines, especially when experimental data are affected by measurement errors or when some data are missing. In this activity, e.g., the valve tumble coefficient was unknown, and the air flow meter was found to provide too high values due to the wrong calibration of the instrument. The procedure adopted in the present activity for the development of the predictive combustion model in GT-Suite is presented in figure 7.

In brief, an imposed combustion model was developed by imposing the experimental heat release data as boundary conditions to provide the input data for the CFD analysis (pressure and temperature values). A closed volume analysis (CPOA, "Cylinder Pressure Only Analysis") was then carried out to evaluate eventual inconsistencies in experimental data, especially concerning volumetric efficiency. To follow, a reverse-run analysis (TPA, "Three Pressure Analysis"), implementing the "EngCylFlow" sub-model, adopting again the experimental pressure data as boundary conditions and targeting the experimental heat release parameters, was performed to calibrate flow field and turbulence model (K-k-ε) constants and valve tumble coefficient. In particular, K-k-ε model constants were found by targeting the TKE and length scale values coming from the 3-D CFD analysis, while CFD tumble number values were used to find the trend of the valve tumble coefficient, experimentally missing. Finally, a premixed turbulent combustion model (SI-Turb, "EngCylCombSITurb") was designed to calibrate the constants of the predictive combustion model by targeting the experimental burn rate trend. A focus on the steps needed for the development of the predictive model is shown in Appendix.

The eight constants to be imposed in the final FR-21T predictive combustion model (which differs from the imposed combustion model for the sole *"EngCylinder"* template) were found by means of an iterative optimization procedure. In detail, the constants C_1, C_2, C_3, and C_T, obtained from the "*EngCylFlow*" analysis, were imposed in the "*Flow Object*" of the final model, while the constants C_λ, C_k, C_S, and *DEM*, found by means of the "*EngCylCombSITurb*" analysis, were set in the "*Combustion Object*". The eight parameters obtained from the calibration process are presented in table 3a and 3b.

Table 3a. Turbulence model coefficients.

Intake Coefficient	C_1	4.07
Production Coefficient	C_2	0.95
Geometric Length Scale Coefficient	C_3	0.62
Tumble Coefficient	C_T	3.14

Table 3b. Combustion model coefficients.

Dilution Exponent Multiplier	*DEM*	1.7
Flame Kernel Growth Multiplier	C_k	8.7
Turbulent Flame Speed Multiplier	C_S	1.2
Taylor Length Scale Multiplier	C_λ	0.8

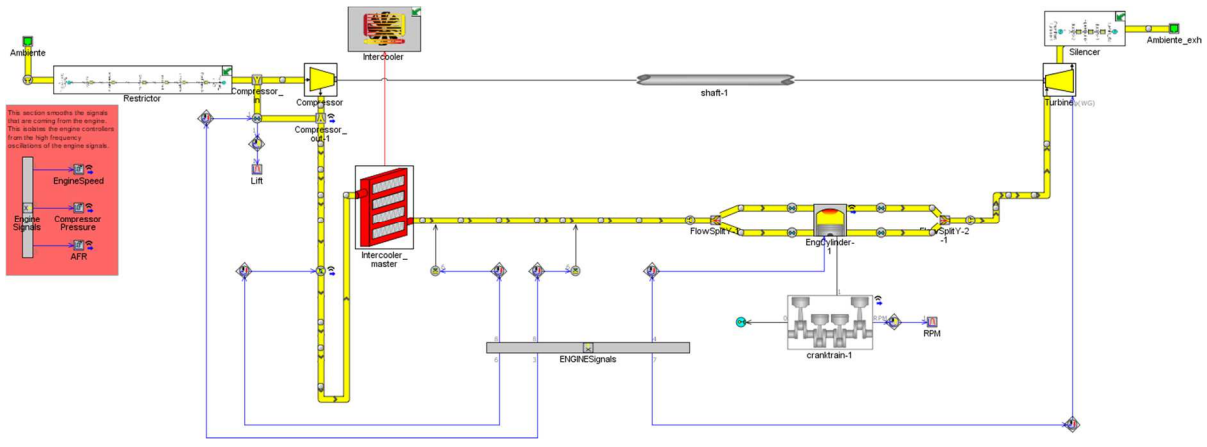

Figure 8. Predictive combustion powertrain model of the FR-21T.

The final FR-21T model, depicted in figure 8, included the whole set of powertrain components.

The predictive model was found able to satisfactorily predict the maximum in-cylinder pressure in the whole operating range, despite a slight underestimation (maximum error of 4.14% at 8150 rpm) with respect to imposed combustion data can be observed between 7600 and 8200 rpm (figure 9a).

Furthermore, from figure 9b it can be observed that the predictive model was found to provide a slightly higher brake mean effective pressure (BMEP) in the whole operating range (maximum error of 2.71% at) as a consequence of the slightly higher volumetric efficiency, which brough to slightly higher values of brake efficiency and brake power at high rotating speed.

Since the maximum relative error of engine performance parameters was always lower than 5%, it can be claimed that the calibration process led to a good description of combustion behaviour.

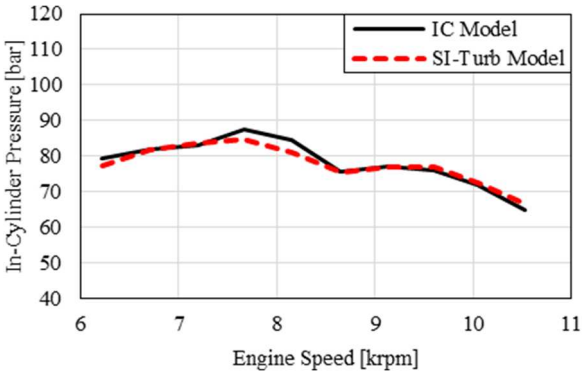

Figure 9a. Max. pressure (predicted/imposed).

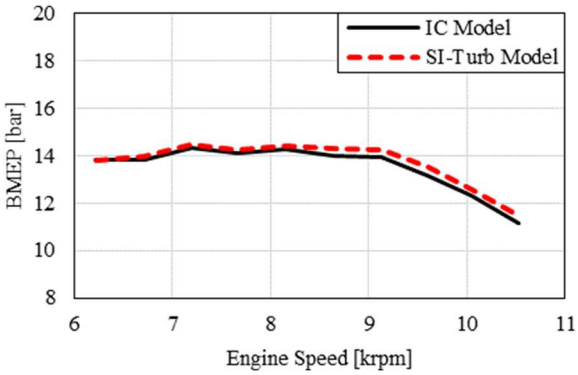

Figure 9b. BMEP (predicted/imposed).

Concerning vehicle modelling, the GT-Suite "*Vehicle Library*" provides a set of standard driveline components and connections. Driveline models are built by means of a combination of 1-D inertias that are linked with either rigid/kinematic connections (one degree of freedom) or slipping/compliant connections (two degrees of freedom). In order to establish the governing motion and the constraint equations of a driveline, GT-Suite adopts the "*Free Driveline Cluster*" model. In order to validate the vehicle model itself (i.e., without engine operation), a numerical coast-down test was carried out and compared to telemetry data. As it can be observed in figure 10, representing a part of the coast down test, the developed vehicle model carefully predicts the telemetry data.

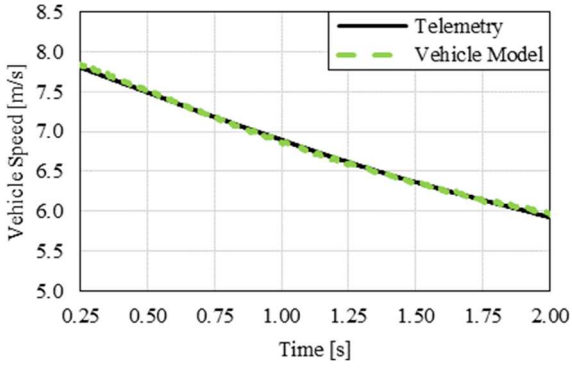

Figure 10. Comparison between telemetry and vehicle model data during coast-down test.

To model the whole EBS-BPV system, the EBS was implemented in the vehicle model by adopting several controls. A pre-calibrated look-up table was used to convert the driver pedal position into volumetric efficiency (VE). The VE signal enters in another pre-calibrated look-up table, in which it is translated in TB opening angle. At the same time, the VE signal enters a third look-up table, establishing the pre-control of the WG (it is worth nothing that the WG pre-control holds the null-load valve closure during pedal release phase), which output is added to that of a PID controller correcting

the pre-control value depending on the actual VE. This PID controller is activated only when target VE exceeds 80% of the achievable VE in wide-open WG conditions (1st-to-2nd region switching).

Concerning the BPV (but also the BOV in the PBS schedule) it is actuated when the pressure drop across the throttle body exceeds 0.8 bar.

3. Results and discussion

In the present section, the benefits of the proposed load control system are evaluated and discussed. The results thus present the comparison between the FR21-T control system (3-region PBS + BOV, marked as PBS-BOV) and that of the future FRT's vehicle (3-region EBS + BPV, denoted as EBS-BPV) in both steady-state conditions, so as to evaluate the benefits in terms of engine efficiency, and in typical FSAE race transient conditions, thus evaluating the prompt response of the vehicle.

3.1. Improvement of the fuel efficiency

Concerning the evaluation of the potential benefits of the EBS-BPV system on engine efficiency, four different steady-state operating conditions, presented in table 4, have been investigated.

As shown in figure 11a, the proposed EBS-BPV system leads to a lower average fuel consumption than the PBS-BOV system in all the investigated cases. This aspect is particularly true at low-load conditions: e.g., a 22.23% lower fuel consumption is obtained in the operating case no. 2 (6210 rpm, 2.05 bar IMEP). The wider opening of the WG in fact significantly reduces the exhaust backpressure, thus reducing the amount of trapped burnt gas at the start of combustion (figure 11b).

Table 4. Steady-state test matrix fore efficiency analysis.

Case [-]	Vehicle speed [km/h]	Gear [-]	Engine speed [rpm]	IMEP [bar]
1	15	3	4120	1.9
2	30	3	6210	2.05
3	45	4	6700	2.7
4	90	4	10050	4.15

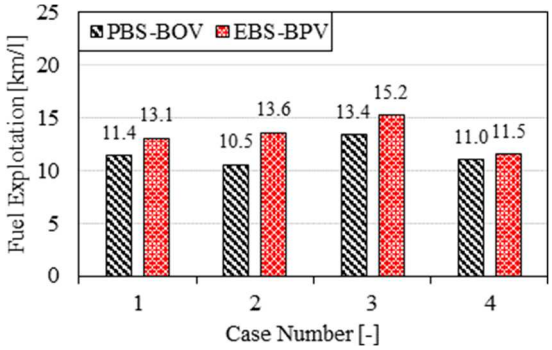

Figure 11a. Average fuel exploitation.

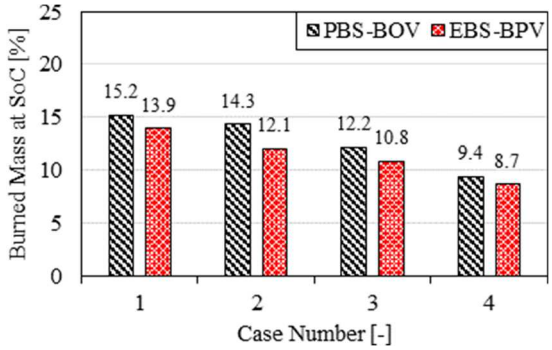

Figure 11b. EGR at Start of Combustion.

Furthermore, pumping losses are significantly decreased by means of the EBS control strategy, as it can be clearly seen, e.g., in the P-V diagram of figure 12 (corresponding to the study case no. 4), resulting in a higher efficiency, and, thus to a lower amount of injected fuel for the same IMEP. This feature has the potential to improve the team rating in the efficiency section of the endurance test.

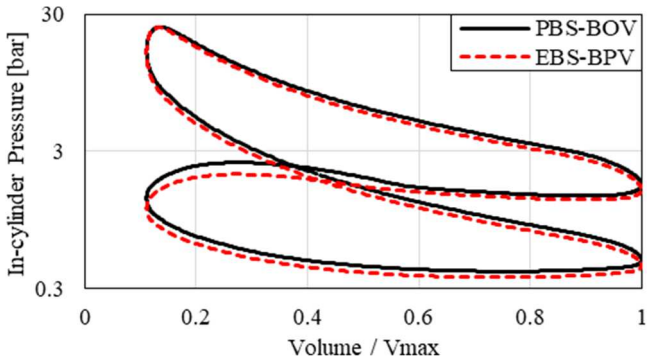

Figure 12. P-V diagram of the case no. 4

3.2. Improvement of the transient response

The potential benefits of the proposed load control system were investigated in a typical FSAE transient behavior. Driver pedal position was imposed in the model by means of a 1-D lookup table as a function of time. In detail, the imposed gas pedal profile (green dashed line in figure 13a) presents at first an initialization period in which gas pedal is fully pushed; then, gas pedal is completely released for few tenths of a second (as in a fast-cornering situation), and fully pushed again. The turbocharger rotating speed, as well as the vehicle speed and the brake power, during the second acceleration phase were observed to evaluate the vehicle performance.

Despite the similarity in the actuation of the BPV and BOV, the PBS-BOV control system brings to a closed WG valve (region 1 in figure 3c) while the BPV, by means of the EBS, manages the WG actuation. In fact, as it can be observed in figure 13b, showing the mass flow rate across the two valves, a lower pressure drop above the TB is required when adopting the proposed control system.

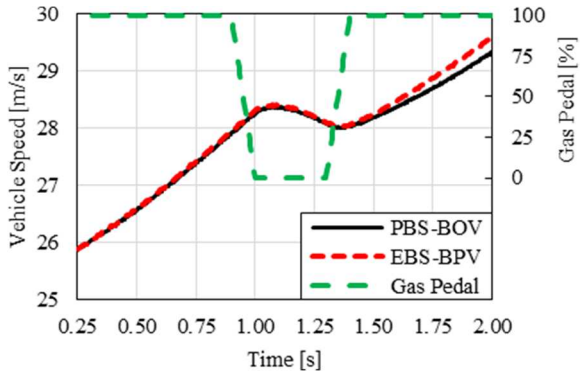

Figure 13a. Vehicle speed and gas pedal.

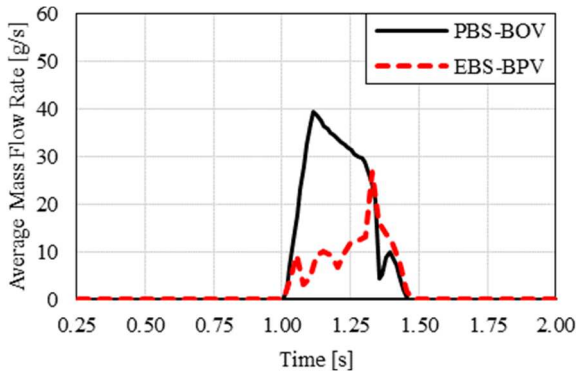

Figure 13b. Mass flow rate crossing valve.

The adoption of the BPV thus brings to a lower decrease of the turbocharger speed during the gas pedal release phase (figure 14a), so that in the next acceleration phase the turbocharger operates at a markedly higher speed, leading to a faster vehicle response (figure 13a).

Furthermore, as it can be observed in figure 14b, the proposed EBS-BPV system brings to an about 3 kW higher engine power in the second acceleration phase of the transient profile, highlighting the advantages, in terms of performance, of the proposed solution.

As a consequence, the travelled distance during the second acceleration phase (0.7 seconds), equals to 20.03 m in the baseline case and 20.15 m when adopting the efficiency-based strategy combined with the BPV, thus showing the potential to bring to a higher score in autocross and endurance tests.

It is worth noting that the reduction of the turbo-lag phenomenon that can be clearly observed in figure 14a not only leads to a better transient response, but also to a higher vehicle drivability, which can be considered a crucial requirement especially in the endurance test (11 km).

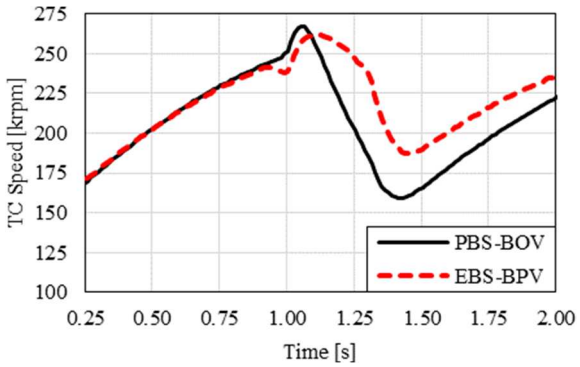

Figure 14a. Turbocharger speed.

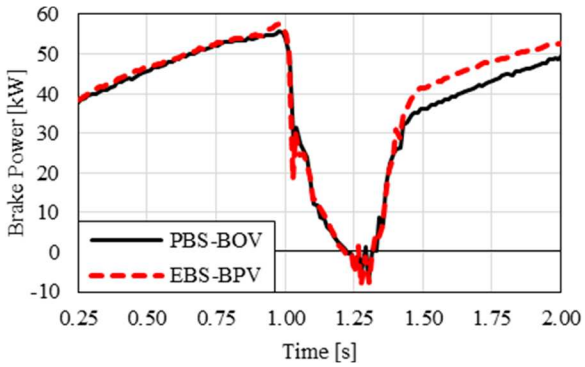

Figure 14b. Engine brake power.

4. Conclusions and final remarks

In spark-ignition turbocharged engines typically engine load is primarily controlled via throttle body (TB), while wastegate valve (WG) only acts to limit boost pressure. To improve the fuel consumption, an efficiency-based strategy (EBS), exploiting WG even at intermediate loads, can be used to reduce pumping losses and exhaust backpressure. Such systems, however, may suffer for a worse transient response and a difficult implementation in motorsport engine control units, such as in Formula SAE.

In this paper, a three-region EBS properly designed for Formula SAE application was proposed. In addition to the smart load control actuation methodology, an anti-lag valve (BPV) was paired (EBS-BPV system) to contemporarily achieve a good transient response and a high powertrain efficiency.

The potential benefits of the proposed solution were evaluated by means of a GT-Suite predictive combustion vehicle model, which development process, including experimental tests at the engine test-bench and 3-D CFD analyses, was widely explained in the paper.

The results show that the proposed EBS-BPV system would bring to the benefits, in terms of fuel usage, coming from the adoption of an efficiency-based strategy (up to 22.23% lower in steady-state conditions), and, at the same time, to the improvement of the transient response thanks to the anti-lag valve (3 kW higher engine power in a fast-cornering situation). Even vehicle drivability improvements were highlighted. The proposed system would thus allow a marked score improvement in FSAE races due to the better performance in the autocross and the improved fuel efficiency and shorter lap time in endurance test.

5. Appendix

The present Appendix aims at describing the step-by-step procedure used to develop the complete FR-21T predictive combustion (PC) model. The calibration procedure, involving the intermediate models, is explained and justified.

5.1. Imposed combustion modelling

An imposed combustion (IC) model of the FR-21T engine was firstly required to provide info about those parts on which no measurements were performed, as well as lately validating the PC model.

The GT-Suite IC modelling follows the two-zone approach:

$$\frac{d(m_u e_u)}{dt} = -p\frac{dV_u}{dt} - Q_u + \left(\frac{dm_f}{dt}h_f\frac{dm_a}{dt}h_a\right) + \frac{dm_{f,i}}{dt}h_{f,i} \quad (1)$$

$$\frac{d(m_b e_b)}{dt} = -p\frac{dV_b}{dt} - Q_b - \left(\frac{dm_f}{dt}h_f\frac{dm_a}{dt}h_a\right) \quad (2)$$

where m_u (m_b) is the unburnt (burnt) zone mass, m_f fuel mass, m_a air mass, $m_{f,i}$ injected fuel mass, e_u (e_b) unburnt (burnt) zone energy, V_u (V_b) unburnt (burnt) zone volume, Q_u (Q_b) unburnt (burnt) zone heat transfer rate, p cylinder pressure, h_f fuel enthalpy, h_a air enthalpy, and $h_{f,i}$ injected fuel enthalpy.

Calibration is carried out by imposing a burn rate profile by means of the Wiebe function, in which the cumulative burn rate normalised to the unit is given from the following equation:

$$\int \frac{dM_b}{d\vartheta} = CE\left(1 - e^{-WC(\vartheta - SOC)^{(E+1)}}\right) \quad (3)$$

where *WC* is the Wiebe constant, *E* Wiebe exponent, *SOC* start of combustion, M_b burnt gas mass, θ crank angle, and *CE* combustion efficiency. Required inputs from indicating measurements concern anchor angle (50% MBF), 10% to 90% MBF duration, combustion efficiency, and Wiebe exponent. The calibration phase provides the "*EngCylCombProfile*" for use in the powertrain model.

The computational domain of the resulting powertrain model is the same of that of the PC (figure 8), including all the components (turbocharger, intercooler, etc.) of the experimental test rig. It is worth noting that turbine and compressor are modelled by means of efficiency maps provided from the supplier. Since each engine condition is described with a specific Wiebe function, the IC powertrain model will provide a linear interpolation of combustion parameters at intermediate conditions.

5.2. Closed volume analysis

A closed volume analysis is not strictly required in the design of a PC model but may be useful to understand potential errors in experimental measurements. In the present study, e.g., the IC model provided volumetric efficiency (VE) values (thus, air mass flow) about 20% lower in average than those evaluated via lambda sensor, whose oxygen values, as known, can be affected by consistent errors. An iterative process involving *Cylinder Pressure Only Analysis* (CPOA) and Wiebe model can be used in GT-Suite to provide information on trapping ratio (usually unknown) and VE; thus, it was used to understand the different behaviour between numerical and measured data.

The CPOA estimates, through a closed volume analysis, the combustion quantities (including burn rate) by using in-cylinder pressure profile, VE, geometries, and averaged wall temperatures. In the Wiebe model instead, the in-cylinder pressure profile is obtained starting from a given burn rate. An optimization procedure was thus carried out by varying VE inside the CPOA until the experimental in-cylinder maximum pressure was matched. The optimization confirmed IC model air mass values, highlighting measurement errors. Thus, the values of air mass flow and VE suggested from the IC model were used instead of experimental data for the next steps.

5.3. Three pressure analysis

The GT-Suite "*Three Pressure Analysis*" (TPA) aims at determining engine quantities difficult to measure directly. Typical TPA outputs are the burn rate, residual fraction, and trapping ratio. TPA is a reverse-run tool, i.e., aimed at calculating the output quantities starting from the measured pressure profiles inside the cylinder, at the cylinder inlet port and at the outlet port, in addition to the start of combustion (SOC, intended as the 0-10% MFB period). Even in this case, the two-zone combustion modelling is adopted. Further details on TPA can be found in [9].

TPA works on a single operating point; thus, the procedure must be repeated for all those relevant engine operating points. In this study, only full-load operating points were available from test bench measurements; thus, the TPA was performed from 6000 to 10500 rpm, by using 500 rpm steps. The domain of the TPA model includes engine cylinder (a single cylinder is used even for multi-cylinder engines), intake and exhaust valves, intake and exhaust ducts, and intake and exhaust ports (figure 15).

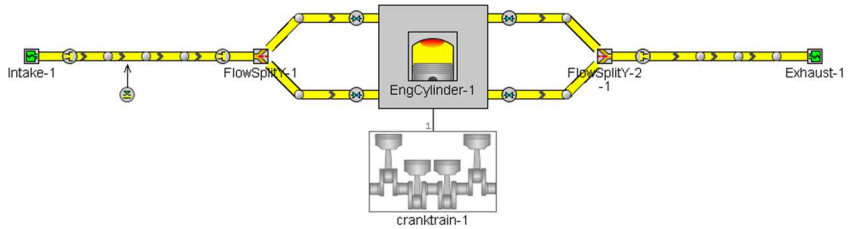

Figure 15. FR-21T engine TPA model.

5.4. Cylinder flow analysis

TPA adds another feature aimed at evaluating flow field parameters and turbulence characteristics inside cylinder, which use is required to develop a PC model. TPA implements the GT-Suite 0-D K-k-ε turbulence model in which three algebraic equations are used to model the behaviour of the mean kinetic energy (K), turbulence kinetic energy (k), and turbulence dissipation rate (ε). The variation of these quantities is described by means of an intake term, an output term, a production term, a tumble term, and finally a dissipation term. These two last terms are not used in the K equation.

$$\frac{d(mK)}{dt} = 0{,}18C_1(1-\alpha_{in})E_{in} + K\dot{m}_{out} - P_k \tag{4}$$

$$\frac{d(mk)}{dt} = 0{,}18C_1\alpha_{in}E_{in} + k\dot{m}_{out} + P_k + C_{Tumb}T - m\varepsilon \tag{5}$$

$$\frac{d(m\varepsilon)}{dt} = 0{,}18C_1E_{in}\frac{\sqrt{k}}{L_g} + \varepsilon\dot{m}_{out} + P_\varepsilon + C_{Tumb}T\frac{\sqrt{k}}{L_g} - 1.92\frac{m\varepsilon^2}{k} \tag{6}$$

This modelling methodology presents several advantages, since it does not require algebraic equations to model the turbulence dissipation rate and the integral length scale, as in the K-k model, and it does not need an algebraic imposed contribution of the mean kinetic energy, as in the k-ε model.

In the GT-Suite K-k-ε approach, four coefficients are used for model calibration. The constant term C_1 is used to calibrate the intake terms in the K and k equations. The constant term C_2 is instead used to calibrate the production term of turbulent kinetic energy P_k and turbulence dissipation P_ε:

$$P_k = 0.38C_2\nu_T\frac{2mK}{{L_g}^2} - \frac{2}{3}mk\left(\frac{\dot{\rho}}{\rho}\right) - \frac{2}{3}m\nu_T\left(\frac{\dot{\rho}}{\rho}\right)^2 \tag{7}$$

$$P_\varepsilon = \frac{\varepsilon}{k}\left[2.19C_2\nu_T\frac{mK}{{L_g}^2} - 2mk\left(\frac{\dot{\rho}}{\rho}\right) - \frac{2.64}{3}m\nu_T\left(\frac{\dot{\rho}}{\rho}\right)^2\right] \tag{8}$$

The constant C_3 evaluates the influence of the geometric length scale (L_g) on the intake term of the k and ε equations:

$$L_g = 0{,}19C_3min(s; 0.5B) \tag{9}$$

Finally, C_{Tumb} acts on the production of turbulence due to the decay of the tumble macro-vortex.

Another critical parameter is the tumble coefficient (C_T) which influences the main kinetic energy in the intake term of all the three equations (E_{in}). C_T should be provided as a function of the crack angle and its knowledge is mandatory.

$$E_{in} = (1-C_T)\frac{1}{2}\dot{m}_{in}{v_{in}}^2 \tag{10}$$

Further information about the GT-Suite K-k-ε model and the sensitivity of the model to the variation of the four parameters can be found in [10] and [11].

In order to calibrate the K-k-ε model, the engine geometries (figure 16), including valves and ports at the bottom dead center (BDC), must be assigned in the TPA reference template.

Figure 16a. Piston surface.

Figure 16b. Head surface.

Then, by activating the "*EngCylFlow*" template and assigning the profile of C_T and the averaged wall temperatures (intake and exhaust ducts, valves, cylinder liner, combustion chamber), the TPA, by means of the assigned pressure profiles, provides an estimation of tumble number, turbulent kinetic energy (TKE), and turbulent length scale as a function of engine °CA. If these quantities are known from a 3-D CFD analysis, an optimization process can be performed in the TPA tool. In fact, the four constants (C_1, C_2, C_3, C_T) can be varied until a desired objective function is minimized. In this study, an integral objective function (ERR) based on TKE and Taylor length scale was used:

$$ERR = \sqrt{\frac{\int_{-180}^{SOC}(k_{0D}-k_{3D})^2 d\vartheta}{k_{avg}(SOC+180)}} + \sqrt{\frac{\int_{-100}^{SOC}(L_{0D}-L_{3D})^2 d\theta}{L_{avg}(SOC+100)}} \quad (11)$$

Where k_{0D} is TKE from the K-k-ε model, k_{3D} TKE from 3-D CFD model, k_{avg} integral average TKE from K-k-ε, L_{0D} the turbulence length scale from K-k-ε model, L_{3D} the turbulence length scale from 3-D CFD model, and L_{avg} the integral average turbulence length scale from K-k-ε.

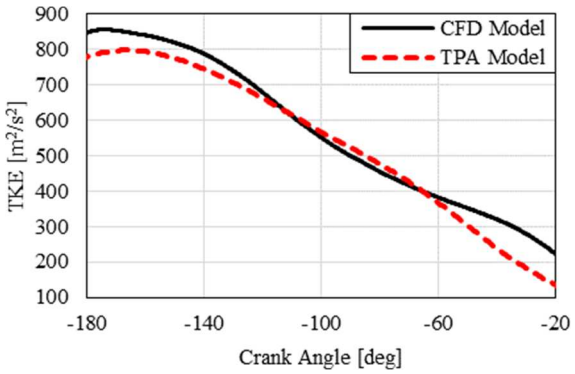

Figure 17a. TKE behaviour (0-D/CFD).

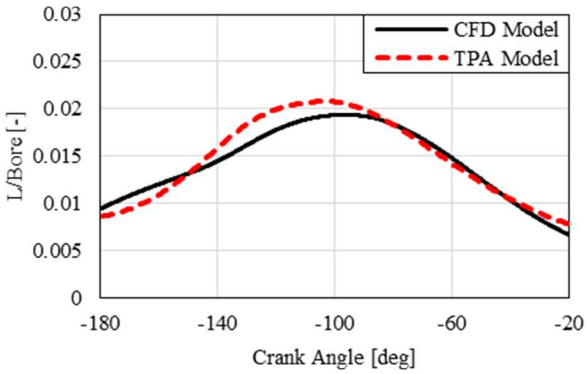

Figure 17b. Turbulence length scale (0-D/CFD).

The optimization domain was set between 0.5 and 5. Three operating conditions at full load were considered: 6000, 8000 and 10000 rpm. Thus, the optimized values are those which minimize the sum of the objective function at the three engine revolutions.

The behavior of the TKE and turbulent length scale obtained by means of the optimization process was satisfactory close to that coming from the 3-D CFD analysis. Figure 17a and figure 17b show, for example, the comparison of turbulence kinetic energy and turbulence length scale at 8000 rpm. The optimized four coefficients of the K-k-ε model are presented in Table 3a.

As already pointed out, the knowledge of the valve tumble coefficient (C_t) as a function of the lift-over-diameter ratio, is crucial to perform the "*EngCylFlow*" analysis, since it influences the intake term of the three K-k-ε equations. C_t represents the ratio of the angular to the linear momentum flux:

$$C_t = \frac{2T_t}{\dot{m}U_{is}D} \quad (12)$$

where T_t is the tumble torque, $\dot{m}$ mass flow rate, U_{is} isentropic valve velocity, and D cylinder bore. U_{is} can be calculated through the equation:

$$U_{is} = \sqrt{RT_0}\left\{\frac{2\gamma}{\gamma-1}\left[1 - P_R^{\frac{\gamma-1}{\gamma}}\right]\right\}^{1/2} \quad (13)$$

where P_R is the static outlet to total inlet pressure ratio, R gas constant, γ specific heat ratio and T_0 specific stagnation temperature.

Thus, the calculation of C_t boils down to the determination of T_t which is typically experimentally determined by means of a paddle wheel flow bench through an impulse meter [12]. In this study a

simplified approach was used since experimental measurements were missing. In detail, the profile of C_t as a function of the lift-over-diameter ratio was supposed to be represented from a S-curve:

$$S(x) = \left(\frac{1}{1+e^{(-kx)}}\right)^a \tag{14}$$

The S-curve profile was validated by observing the C_t profile of a similar cylinder [13].

An optimization procedure was set in the TPA "*EngCylFlow*" tool varying the two parameters *a* and *k* of the S-curve equation. An objective function was built to achieve the same tumble number profile resulting from the already mentioned 3-D CFD analysis.

$$ERR_T = \sqrt{\frac{\int_{-270}^{-170}(Tumb_{0D}-Tumb_{3D})^2 d\theta}{Tumb_{avg}(-170+270)}} \tag{15}$$

where $Tumb_{0D}$ is the tumble number from K-k-ε model, $Tumb_{3D}$ the tumble number from 3-D CFD model, and $Tumb_{avg}$ the integral average tumble number from K-k-ε.

This operation was iteratively performed by alternating to the K-k-ε calibration procedure until convergence was achieved. The calibration procedure of the S-curve provided optimal values of 10.1 for the constant *k* and 25.1 for *a*.

5.5. Turbulent spark ignition combustion model

The PC model of GT-Suite is set by activating the "*EngCylCombSITurb*" (SI-Turb) function. The SI-Turb model aims at predicting the behaviour of the burn rate in the whole operating range in premixed SI engines (carburettor and PFI). The SI-Turb is a two-zone combustion model in which the behaviour of the burnt gas is evaluated through the following equations:

$$\frac{dM_e}{dt} = \rho_u A_e (S_L + S_T) \tag{16}$$

$$\frac{dM_b}{dt} = \frac{(M_e - M_b)}{\tau} \tag{17}$$

where M_e is the entrained unburnt mixture mass, M_b the burnt gas mass, τ the time constant, S_L the laminar flame speed, S_T the turbulent flame speed, A_e the surface area at the edge of the flame front, and ρ_u the unburnt mixture density.

The first equation states that the unburned fuel-air mixture is entrained into the flame front through the flame area at a rate proportional to the sum of the turbulent and laminar flame speeds. During the first flame kernel development phase, the mixture entrainment is limited by the laminar flame speed, which depends on pressure, temperature, air-to-fuel ratio, and residual gas.

$$S_L = (B_m + B_\Phi(\Phi - \Phi_m)^2)\left(\frac{T_u}{T_0}\right)^\alpha \left(\frac{p}{p_0}\right)^\beta f(Dil) \tag{18}$$

$$f(Dil) = (1 - 2.06 Dil^{0.77DEM}) \tag{19}$$

where B_m is the maximum laminar speed, B_Φ the laminar speed roll-off value, Φ the equivalence ratio, Φ_m the equivalence ratio at maximum speed, T_U the unburnt mixture temperature, T_0 the reference temperature (298 K), p the in-cylinder pressure, p_0 the reference pressure (101325 Pa), *Dil* the residual mass fraction in the unburnt zone, and *DEM* the dilution effect multiplier.

Then, the turbulent contribute is added to the laminar term to find the fresh mixture entrainment:

$$S_T = C_S u' \left(1 - \frac{1}{1+C_k\left(R_f^2\right)/\left(L_t^2\right)}\right) \tag{20}$$

where R_f is the flame radius, L_t the turbulence length scale, and *u'* the turbulence intensity.

The transition between laminar and turbulent flame speed is evaluated from the equation of the turbulent flame speed itself through the flame kernel growth multiplier (C_k) scaling the flame front

evolution from an initial smooth surface to a fully developed turbulent wrinkled flame. The turbulent flame speed multiplier (C_S) instead scales the contribute of the turbulent flame speed to the mixture entrainment.

The second equation instead states that the burn rate across the flame front is proportional to the difference between the burned and unburned mixtures. The time constant (τ) is defined as the time required to the laminar flame speed to cover the Taylor microscale (λ) assuming isotropic turbulence:

$$\tau = \frac{\lambda}{S_L} \tag{21}$$

$$\lambda = C_\lambda \frac{L_t}{Re_t^{1/2}} \tag{22}$$

where Re_t is the turbulent Reynolds number, and C_λ is the Taylor length scale multiplier.

In the Taylor microscale equation, C_λ aims at calibrating the slope of the burn rate profile: the higher C_λ, the higher instantaneous burn rate.

Thus, the development of a reliable PC model for SI PFI engines in GT-Suite requires the proper calibration of the four constants C_λ, C_k, C_S, and *DEM*. Further information about the sensitivity of these parameters on the burn rate profile can be found in [14]. To calibrate the four constants, a "*Measured+Predicted*" (M+P) analysis is required. The M+P model carries out a CPOA providing a comparison of the in-cylinder pressure and the burn rate between experimental data and model output. The "*EngCylInit*" template is used to initialize in-cylinder quantities. Values coming from TPA results concerning VE and fuel mass at inlet valve closing are used in input, together with trapping ratio, residual fraction, and turbulence level. Other inputs concern combustion chamber geometry and spark plug location.

The calibration process aims at finding the constants best matching the numerical and experimental combustion quantities in a wide number of operating points. Target quantities depend on the objective function; in this study, the "*Improved Burn Rate RMS Error*" (from RLT variables), was used:

$$IBR = \sqrt{\frac{\int_{t_0}^{t_f} (LHV_{pred} BR_{pred} - BR_{meas})^2 dt}{t_f - t_0}} \tag{23}$$

where LHV_{pred} is the LHV multiplier (from the predicted burn rate), BR_{pred} is the predicted burn rate, and BR_{meas} is the measured burn rate. The optimization domain of the parameters was set between 0.5 and 3, except for C_k for which the upper constraint was set to 10, as suggested in [10]. Engine operating conditions at full load were considered, from 6000 to 10500 rpm.

Figure 18a, e.g., compares the behaviour of the predicted in-cylinder pressure to that measured at the test bench at 8000 rpm. Figure 18b instead compares the slope of the burn rate at the same speed.

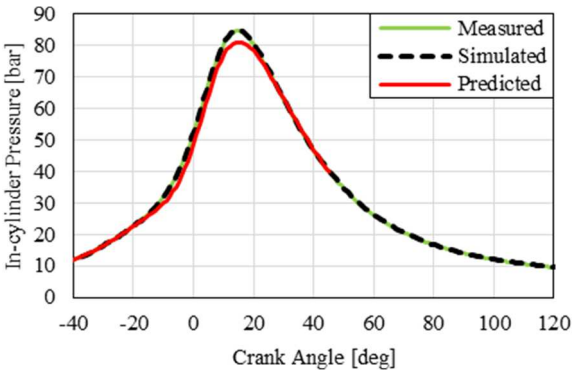

Figure 18a. Pressure trend, 8 krpm (0-D/CFD).

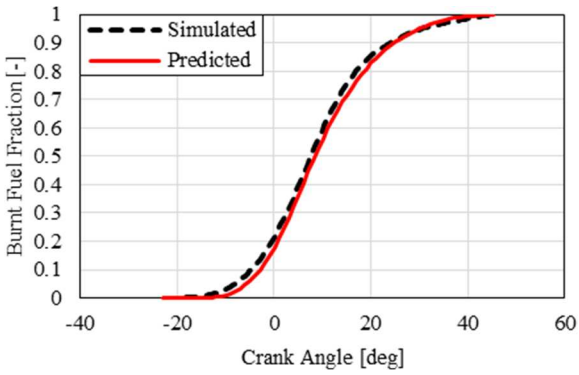

Figure 18b. S-curve, 8 krpm (0-D/CFD).

The optimized four coefficients of the "*EngCylCombSITurb"* model are presented in Table 3b.

References

[1] Vignesh Kumar M and Murugesan S 2018 Analysis and Development of Restrictor for Parallel Twin Engine in FSAE Cars *Int. J. Eng. Technol.* **7** 311–4
[2] Shinde P A 2014 Research and optimization of intake restrictor for Formula SAE car engine *IJSRP* **4** 1–5
[3] Claywell M and Horkheimer D 2006 Improvement of Intake Restrictor Performance for a Formula SAE Race Car through 1D & Coupled 1D/3D Analysis Methods *SAE Technical Paper 2006-01-3654* 1–27
[4] Bosi L, Ciampolini M, Romani L, Balduzzi F and Ferrara G 2020 Experimental Analysis on the Effects of Passive Prechambers on a Small 2-Stroke Low-Pressure Direct Injection (LPDI) Engine *SAE Technical Paper 2020-32-2305* 1–11
[5] Ciampolini M, Fazzini L, Berzi L, Ferrara G and Pugi L 2020 Simplified Approach for Developing Efficiency Maps of High-Speed PMSM Machines for Use in EAT Systems Starting from Single-Point Data *2020 IEEE International Conference on Environment and Electrical Engineering and 2020 IEEE Industrial and Commercial Power Systems Europe (EEEIC / I CPS Europe)* (Madrid, ES) 1–6
[6] Eriksson L, Frei S, Onder C and Guzzella L 2002 Control and Optimization of Turbocharged Spark Ignited Engines *IFAC Proceedings Volumes* **35** 283–8
[7] Gorzelic P, Hellstrom E, Stefanopoulou A, Jiang L and Gopinath S 2012 A coordinated approach for throttle and wastegate control in turbocharged spark ignition engines *2012 24th Chinese Control and Decision Conference* (Taiyuan, CN) 1524–9
[8] Nazari S, Stefanopoulou A, Kiwan R and Tsourapas V 2016 A Coordinated Boost Control in a Twincharged Spark Ignition Engine with High External Dilution *Proc. ASME 2016 Dynamic Systems and Control Conference* (Minneapolis, USA) 1–8
[9] Mirzaeian M, Millo F and Rolando L 2016 Assessment of the Predictive Capabilities of a Combustion Model for a Modern Downsized Turbocharged SI Engine *SAE Technical Paper 2016-01-0557* 1–10
[10] Toman R and Macek J 2017 Evaluation of the Predictive Capabilities of a Phenomenological Combustion Model for Natural Gas SI Engine *MECCA* **02** 37–48
[11] Fogla N, Bybee M, Mirzaeian M, Millo F and Wahiduzzaman S 2017 Development of a K-k-∈ Phenomenological Model to Predict In-Cylinder Turbulence *SAE Int. J. Engines* **10** 1–14
[12] El-Adawy M, Heikal M, A. Aziz A, Siddiqui M and Munir S 2017 Characterization of the Inlet Port Flow under Steady-State Conditions Using PIV and POD *Energies* **10** 1–16
[13] Masi M, Artico L and Gobbato P 2019 Study on the reliability of paddle-wheel tumble flow meters for high-speed engines *AIP Conference Proceedings* 2191 (Erode, IN)
[14] Robertson D, Conway G, Chadwell C, McDonald J, Barba D, Stuhldreher M and Birckett A 2018 Predictive GT-Power Simulation for VNT Matching on a 1.6 L Turbocharged GDI Engine *SAE Technical Paper 2018-01-0161*